

PLENARY TALK

## Strategies for baryon resonance analysis

To cite this article: M. Döring *et al* 2009 *Chinese Phys. C* **33** 1127

View the [article online](#) for updates and enhancements.

### Related content

- [A Pedagogical Introduction to Electroweak Baryogenesis: The baryon asymmetry](#)  
G A White
- [A Pedagogical Introduction to Electroweak Baryogenesis: Introduction](#)  
G A White
- [Baryon resonance analysis from SAID](#)  
R. A. Arndt, W. J. Briscoe, M. W. Paris et al.

# Strategies for baryon resonance analysis<sup>\*</sup>

M. Döring<sup>1</sup> C. Hanhart<sup>1,2</sup> HUANG Fei(黄飞)<sup>3</sup> S. Krewald<sup>1,2;1)</sup> U.-G. Meißner<sup>1,2,4</sup>

1 (Institut für Kernphysik and Jülich Center for Hadron Physics, Forschungszentrum Jülich, D-52425 Jülich, Germany)

2 (Institute for Advanced Simulation, Forschungszentrum Jülich, D-52425 Jülich, Germany)

3 (Department of Physics and Astronomy, University of Georgia, Athens, Georgia 30602, USA)

4 (Helmholtz-Institut für Strahlen- und Kernphysik (Theorie) and Bethe Center for Theoretical Physics, Universität Bonn, Nußallee 14-16, D-53115 Bonn, Germany)

**Abstract** The analytic properties of scattering amplitudes provide a meeting point for experimental and theoretical investigations of baryon resonances. Pole positions and residues allow for a parameterization of resonances in a well-defined way which relates different reactions. The recent progress made within the Jülich model is summarized.

**Key words** pion-nucleon scattering, meson exchange model, analytic structure of the scattering amplitude

**PACS** 14.20.Gk, 13.75.Gx, 11.80.Gw

## 1 Introduction

Currently, there is rapid progress in experimental investigations of the baryon resonance spectrum up to center of mass energies of 3 GeV. In this energy region, resonances which couple to many decay channels, in particular multi-pion final states, may have large widths, and overlap. For photon-induced reactions, complete experimental studies of the polarization degrees of freedom are being performed in order to resolve ambiguities in the partial wave analysis. Unfortunately, no systematic investigations of the polarization dependence of the pion-nucleon reaction are available in this energy range, which makes an improvement of the classical partial wave analyses by Cutkosky, Höhler and Arndt and collaborators difficult<sup>[1–5]</sup>.

The extraction of resonance parameters from a given partial wave analysis has to provide a separation of the partial wave amplitude into a resonant and non-resonant part. Here we want to study that separation within the framework of a theoretical approach based on effective Lagrangians, such as<sup>[6–8]</sup>. The present contribution focusses on recent results obtained within the Jülich model<sup>[9–13]</sup>. The Jülich

model is a coupled channel approach which includes effective two-pion nucleon channels in addition to the pion-nucleon and the eta-nucleon channels. The analytical structure of the model allows continuation into the complex plane.

## 2 Resonance analysis within the Jülich model

At a first glance, a theoretical model appears to have no difficulty in distinguishing a background contribution from a resonance contribution. Starting from a field-theoretical Lagrangian, there is a unique way to classify diagrams into one-line reducible and irreducible ones. The bare interaction can be split into so-called pole diagrams and non-pole diagrams. The iteration of the non-pole diagrams in the Lippmann-Schwinger equation results in what commonly is called the non-pole  $T$ -matrix. Given the non-pole  $T$ -matrix, one proceeds to compute dressed vertices and self energies. Ultimately, one achieves to split the exact  $T$ -matrix into a non-pole and a pole part:

$$T = T^{\text{NP}} + T^{\text{P}}. \quad (1)$$

Received 7 August 2009

<sup>\*</sup> Supported by DFG (Deutsche Forschungsgemeinschaft, Gz: DO 1302/1-1), Helmholtz Association through funds provided to the virtual institute “Spin and Strong QCD” (VH-VI-231), EU-Research Infrastructure Integrating Activity “Study of Strongly Interacting Matter” (HadronPhysics2, grant n. 227431) under the Seventh Framework Program of EU and DFG (TR 16), COSY FFE grant No. 41445282 (COSY-58)

1) E-mail: s.krewald@fz-juelich.de

©2009 Chinese Physical Society and the Institute of High Energy Physics of the Chinese Academy of Sciences and the Institute of Modern Physics of the Chinese Academy of Sciences and IOP Publishing Ltd

The construction of  $T^P$  is summarized in Fig. 1.

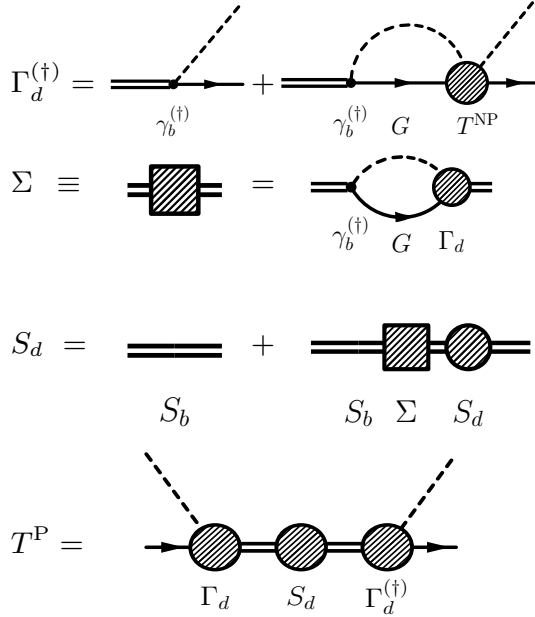


Fig. 1. Theoretical  $T$ -matrix: Pole and Non-pole contributions.

On the other hand, the  $S$ -matrix is uniquely characterized by its analytical structure. In order to extract the pole residue, we expand the amplitude  $T^{(2)}$  on the second sheet in a Laurent series around the pole position,

$$T^{(2) i \rightarrow j} = \frac{a_{-1}^{i \rightarrow j}}{z - z_0} + a_0^{i \rightarrow j} + \mathcal{O}(z - z_0), \quad (2)$$

where  $i$  and  $j$  denote the various channels considered. In the following, we compare the theoretical decomposition into pole and non-pole diagrams, Eq. (1) with the one based on Eq. (2). Fig. 2 shows the partial wave amplitude for the  $P_{33}$  partial wave. The full solution of the Jülich model (solid red line) agrees with the Arndt solution<sup>[5]</sup>. Adding the pole contribution  $\frac{a_{-1}}{z - z_0}$  to the non-pole  $T$ -matrix produces a drastic deviation from the amplitude of the full solution (dashed-dotted black line). The reason for this behavior can be traced to the fact that the pole  $T$ -matrix is an analytic function by itself which has a non-trivial polynomial contribution in addition to the pole term. Explicitly, the residue reads

$$a_{-1} = \frac{\Gamma_d \Gamma_d^{(\dagger)}}{1 - \frac{\partial}{\partial Z} \Sigma}, \quad (3)$$

whereas the polynomial part starts with the constant:

$$a_0 = T^{\text{NP}} + a_0^P. \quad (4)$$

The pole  $T$ -matrix contributes:

$$a_0^P = \frac{a_{-1}}{\Gamma_d \Gamma_d^{(\dagger)}} \left( \frac{\partial}{\partial Z} (\Gamma_d \Gamma_d^{(\dagger)}) + \frac{a_{-1}}{2} \frac{\partial^2}{\partial Z^2} \Sigma \right). \quad (5)$$

Adding the constant defined by Eq. (4) to the actual pole contribution, or in other words, using Eq. (2), one obtains a reasonable approximation to the full calculation (dashed red line). As one moves away from the pole energy, the higher powers of the polynomial expansion become increasingly important, of course. A partial cancellation in  $a_0$  of the contributions of the non-pole  $T$ -matrix  $T^{\text{NP}}$  and the pole  $T$ -matrix  $T^P$  is observed not only for the  $P_{33}$ , but also for most of the other energetically low-lying resonances. Fig. 2 demonstrates that a separation of a global smooth background, such as the one given by the non-pole  $T$ -matrix (blue solid line), from the experimental data may be misleading.

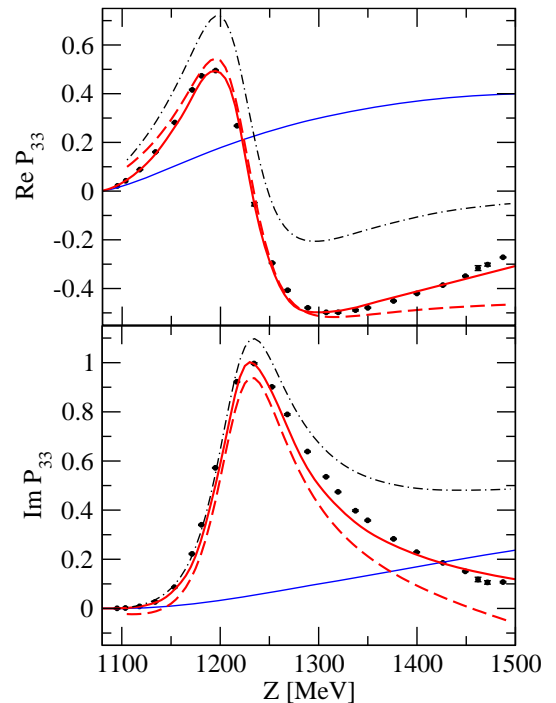


Fig. 2. The  $P_{33}$  partial wave amplitude, decomposed into real (upper figure) and imaginary (lower figure) parts. The Jülich model is given by the solid (red) line. The dashed-dotted and dashed lines refer to two approximations discussed in the text.

There is another observation to be made in connection with so-called dynamically generated resonances. As is known from Chew-Low theory, the  $u$ -channel Born diagram in the  $P_{33}$  partial wave for pion nucleon scattering generates attraction. After iteration, the corresponding  $T$ -matrix may have a pole on the second Riemann sheet, see Fig. 3, blue surface.

The residue of that pole is canceled, once a bare pole is added, and the pole of the full amplitude is at the physical position (red surface) while the pole visible in  $T^{\text{NP}}$  has moved far away into the complex plane. This observation shows that conclusions concerning the nature of resonances should be made only after a quantitative fit to the data has been achieved.

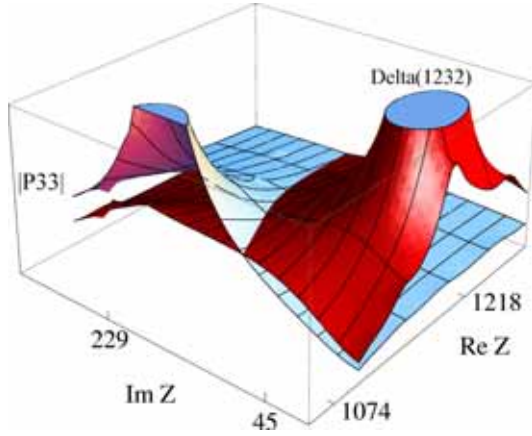


Fig. 3. The second Riemann sheet of the  $P_{33}$  partial wave amplitude. The red surface shows the magnitude of the amplitude evaluated in the full Jülich model. The blue surface represents the amplitude generated by the non-pole  $T$ -matrix.

### 3 Resonance interference in $S_{11}$

The  $S_{11}$  partial wave is of particular interest because there are two resonances in this partial wave.

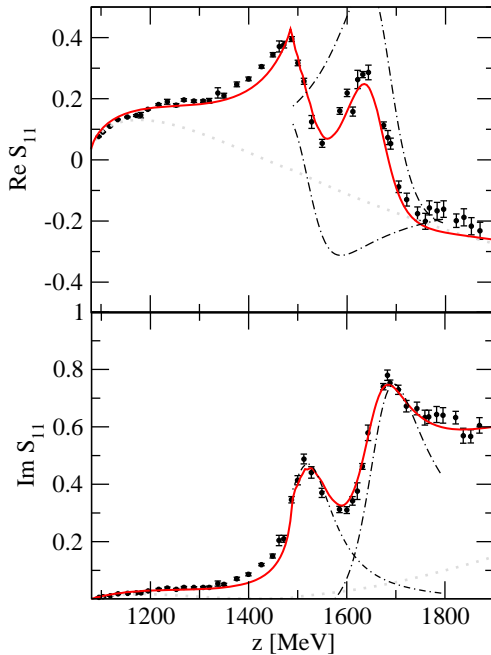


Fig. 4. Amplitude in the  $S_{11}$  partial wave. See text for legend.

In Fig. 4, the partial wave amplitude of the  $S_{11}$  partial wave is plotted. The full solution of the Jülich model is indicated with the solid red lines. It describes well the SES solution of Ref. [5] up to  $z \sim 1.9$  GeV. The gray dotted lines indicate  $T^{\text{NP}}$ . We can also plot the pole approximation from Eq. (2). For simplicity, we set  $a_0 = 0$ . On the physical axis, the pole approximations of the  $N^*(1535)$  and  $N^*(1650)$  appear as resonant like structures indicated with the black dashed-dotted lines.

At first sight, the shapes of the real parts of the partial wave amplitudes of the two resonances are quite different: While the pole approximation of the  $N^*(1535)$  shows a familiar shape with a maximum and a minimum in  $\text{Re } S_{11}$ , the  $N^*(1650)$  looks quite different. The reason is that  $a_{-1}$  is a complex number that mixes real and imaginary parts of a classical Breit-Wigner shape. In other words, the phase of the resonances is responsible for this twisting of resonance shapes and can have a very large effect.

The individual contributions from the two resonances (black dashed-dotted lines) are quite different from the full solution. However, the sum

$$T_a^{(2)}(z) = \frac{a_{-1}^{N^*(1535)}}{z - z_0^{N^*(1535)}} + \frac{a_{-1}^{N^*(1650)}}{z - z_0^{N^*(1650)}}, \quad (6)$$

indicated as the purple dashed lines in Fig. 5, fits the full solution quite well over the entire resonance region.

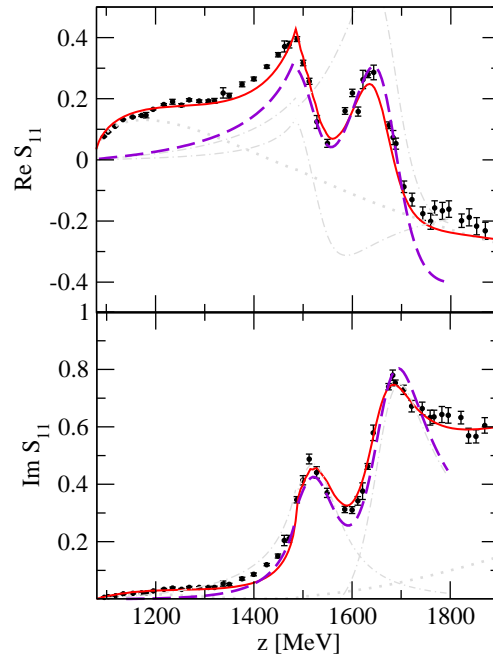


Fig. 5. The purple dashed line shows the sum of pole approximations (dashed dotted lines) from two different sheets that are connected to the physical axis below and above the  $\eta N$  threshold, respectively.

Thus, the two resonances cannot be treated separately but must be treated together; the residue from the  $N^*(1535)$  provides a strongly energy dependent background in the  $N^*(1650)$  region and viceversa. Note that the real part of the partial wave amplitude shows a strong energy dependence of the tail of the  $N^*(1535)$  in the region of the  $N^*(1650)$ . The resonances interfere with each other.

For a theoretical description one needs a unitary coupled channel model like the present one, which also allows for resonance interference. Otherwise, if one tries to extract resonance parameters individually for each resonance, one needs a substantial phenomenological background. Then, the parameters depend very strongly on that particular background and results are not reliable.

So far, only the pole structure above the  $\eta N$  cusp has been discussed. At energies above  $z = m_\pi + m_\eta$ , the physical axis is directly connected to the Riemann sheet, where the physical poles have been analysed. This sheet is the unphysical one with respect to the  $\pi N$  and the  $\eta N$  channel, called sheet 22 in Fig. 6. Sheet 21 is the second sheet to the  $\pi N$  channel, but a physical sheet with respect to the  $\eta N$  channel.

The physical  $N^*(1535)$  and  $N^*(1650)$  are on sheet 22, but on sheet 21, there are hidden poles. As a result a prominent cusp in the amplitude becomes visible.

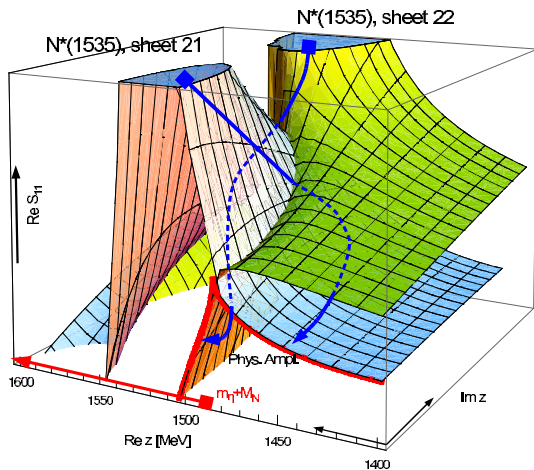


Fig. 6. Impact of poles on different sheets on the physical amplitude.

A full discussion of the poles and residues obtained in the Jülich model will be presented in the talk by M. Döring<sup>[14]</sup>. In the limit of high excitation energies, cross sections become forward peaked and show a smooth energy dependence. The implications of the physics above 3 GeV for the resonance analysis<sup>[15]</sup> are discussed in the talk by F. Huang<sup>[16]</sup>.

## 4 Quark mass dependence

Lattice calculations of the nucleon octet are relatively straightforward to perform because the lattice approach emphasizes the ground state of a given system, but suppresses the excitation modes. Despite these difficulties, first lattice investigations of the excited states of the nucleon have become available both for the positive and negative parity excitations. Recently, new techniques have been proposed how to extract even the second and third excited states of a given multipolarity<sup>[17]</sup>. Lattice calculations do not use quark masses consistent with the physical mass of the pion. For technical reasons, much larger quark masses have to be used. The results obtained for a set of large quark masses are extrapolated to the experimental pion mass. It turns out that the extrapolation deviates from a straight line. Chiral perturbation theory offers a possibility to study the quark mass dependence of the nucleon mass within a controlled theoretical framework, see for example Ref. [18]. Applications of this formalism to the masses of the Roper resonance<sup>[19]</sup> and the  $\Delta_{33}$ <sup>[20]</sup> are available.

Within the present approach, a link to the quark mass dependence of the resonance masses is not possible. Nevertheless we can vary the pion mass in the pion-nucleon propagator and study the sensitivity of the pole positions of the resonances on the pion mass. For sufficiently large pion masses, the multi-pion final channels close. A variation of the pion mass therefore corresponds to a modification of the final state interaction. In Fig. 7, we show the real part of the pole position of resonances on the pion mass. In the case of the  $P_{33}$  resonance, the present approach introduces a relatively strong modification due to final state interactions, as shown in Fig. 3. The non-pole  $T$ -matrix by itself is able to generate a pole, although not at the correct physical energy. Indeed, one finds an increase of the mass of the  $P_{33}$  of about 50 MeV, when the pion mass is increased from 140 MeV to 280 MeV. Many authors have claimed that the  $N^*(1535)$  is generated by Kaon Lambda and Kaon Sigma dynamics, see e.g. Ref. [21]. Fig. 7 shows a strong sensitivity of the  $N^*(1535)$  to meson-nucleon dynamics already when taking into account only the  $\eta N$  and the effective two-pion nucleon channels. An extension of the present model to include channels with strange particles is in preparation. Quite surprisingly, the  $N^*(1650)$  remains virtually unaffected by the changes of the pion mass. The width of the  $N^*(1650)$  strongly decreases with increasing pion mass, however, see Fig. 8. The present investigation shows that the  $N^*(1650)$  might

be particularly interesting for lattice studies, as its mass appears to be stable against modifications of the final state interaction due to changes of the pion mass. Eventually, a matching of the low-energy limit of the present approach to chiral perturbation theory may make possible quantitative comparisons with lattice results.

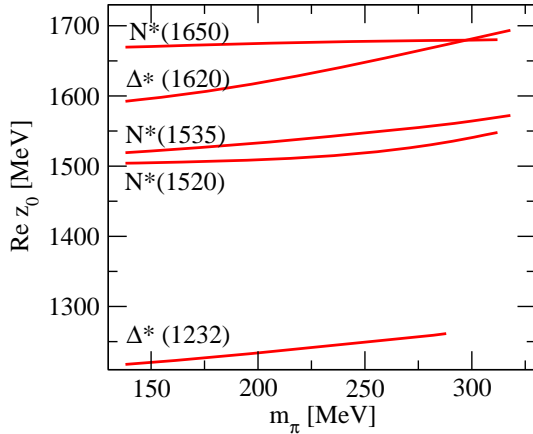


Fig. 7. Real part of the pole position as a function of  $m_\pi$  for various resonances.

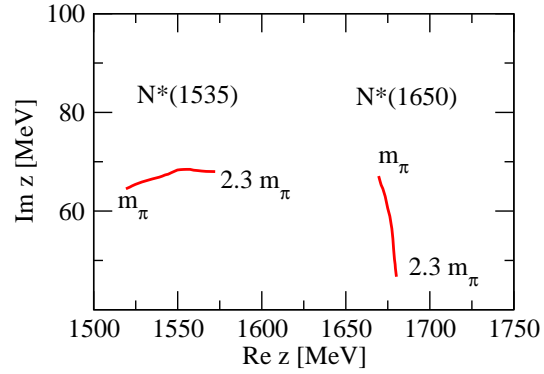


Fig. 8. Trajectories of the  $N^*(1535)$  and  $N^*(1650)$  poles in the complex  $z$  plane as a function of  $m_\pi$ .

## 5 Conclusions

The analytical structure of the meson-nucleon  $T$ -matrix offers a meeting point for theoretical and experimental baryon resonance analysis. We have extracted the poles and the zeroes of the  $T$ -matrix in the various Riemann sheets, and obtained the corresponding residues within the Jülich model.

## References

- 1 Arndt R A, Briscoe W J, Strakovsky I I, Workman R L. Phys. Rev. C, 2006, **74**: 045205
- 2 Höhler G.  $\pi N$  Newsletter, 1993, **9**: 1
- 3 Cutkosky R E, Forsyth C P, Hendrick R E, Kelly R L. Phys. Rev. D, 1979, **20**: 2839
- 4 Arndt R A, Briscoe W J, Strakovsky I I, Workman R L, Pavan M M. Phys. Rev. C, 2004, **69**: 035213
- 5 Arndt R A, Briscoe W J, Strakovsky I I, Workman R L R. Arndt, Briscoe W, Strakovsky I, Workman R. Eur. Phys. J. A, 2008, **35**: 311
- 6 Shklyar V, Lenske H, Mosel U, Penner G. Phys. Rev. C, 2005, **71**: 055206; **72**: 019903
- 7 Sato T, Lee T-S H. Phys. Rev. C, 1996, **54**: 2660
- 8 Julia-diaz B, Lee T-S H, Matsuyama A, Sato T. Phys. Rev. C, 2007, **76**: 065201
- 9 Schutz C, Haidenbauer J, Speth J, Durso J W. Phys. Rev. C, 1998, **57**: 1464
- 10 Krehl O, Hanhart C, Krewald S, Speth J. Phys. Rev. C, 2000, **62**: 025207
- 11 Gasparyan A M, Haidenbauer J, Hanhart C, Speth J. Phys. Rev. C, 2003, **68**: 045207
- 12 Döring M, Hanhart C, HUANG F, Krewald S, Mei  $\beta$  ner U-G. Phys. Lett. B has been accepted
- 13 Döring M, Hanhart C, HUANG F, Krewald S, Mei  $\beta$  ner U-G. Nucl. Phys. A, 2009, 170
- 14 Döring M. Talk at the Workshop on the Physics of Excited Nucleon — NSTAR2009, Beijing April 19 — 22, 2009
- 15 HUANG F, Sibirtsev A, Krewald S, Hanhart C, Haidenbauer J, Mei  $\beta$  ner U-G. Eur. Phys. J. A, 2008, **40**: 311
- 16 HUANG F. Talk at the Workshop on the Physics of Excited Nucleon — NSTAR2009, Beijing April 19 — 22, 2009
- 17 Fleming G T, Cohen S D, LIN H W, Pereyra V. arXiv:0903.2314 [hep-lat]
- 18 Mei  $\beta$  ner U-G, PoS LAT 2005:009,2006; arXiv:0509029 [hep-lat]
- 19 Borasoy B, Bruns P C, Mei  $\beta$  ner U-G, Lewis R. Phys. Lett. B, 2006, **641**: 294
- 20 Bernard V, Hoja D, Mei  $\beta$  ner U-G, Rusetsky A. JHEP, 2009, **06**: 061
- 21 Kaiser N, Siegel P B, Weise W. Phys. Lett. B, 1995, **362**: 23